Optics and Lasers in Engineering 49 (2011) 618–622

Contents lists available at ScienceDirect

Optics and Lasers in Engineering

journal homepage: www.elsevier.com/locate/optlaseng

Calculation of the frequency response in step-index plastic optical fibers using the time-dependent power flow equation

Branko Drljača [a], Svetislav Savović [a,*], Alexandar Djordjevich [b]

[a] Faculty of Science, R. Domanovića 12, 34000 Kragujevac, Serbia
[b] City University of Hong Kong, 83 Tat Chee Avenue, Kowloon, Hong Kong, China

ARTICLE INFO

Article history:
Received 25 October 2010
Received in revised form
17 January 2011
Accepted 18 January 2011
Available online 5 February 2011

Keywords:
Plastic optical fiber
Frequency response
Bandwidth

ABSTRACT

The time-dependent power flow equation, which is reduced to its time-independent counterpart is employed to calculate frequency response and bandwidth in addition to mode coupling and mode-dependent attenuation in a step-index plastic optical fiber. The frequency response is specified as a function of distance from the input fiber end. This is compared to reported measurements. Mode-dependent attenuation and mode dispersion and coupling are known to be strong in plastic optical fibers, leading to major implications for their frequency response in data transmission systems.

1. Introduction

Plastic optical fibers (POFs) are often considered for high-performance short-distance data transmission systems including high-bandwidth local-area networks and multi-node bus networks [1–4]. In addition to being a more affordable, flexible and rugged alternative to glass fibers, POFs are also easier to handle. Their large-core diameter (0.5–1 mm or larger) allows pairing with LED sources using low-precision plastic components. This results in inexpensive but robust systems that are easy to interconnect. Variety of POF applications have been commercialized ranging from simple light-transmission guides in displays and power delivery systems to sensors and short-haul communication links [4]. Installations within buildings or vehicles, where sharp corners and branches are many or the network is repeatedly reconfigured, represent a domain with growth potential for POF applications.

Transmission properties of step-index (SI) multimode optical fibers, such as frequency response and bandwidth, depend strongly upon mode-dependent attenuation, modal dispersion and the rate of mode coupling (power transfer from lower to higher order modes) caused by intrinsic perturbation effects (primarily due to microscopic bends, irregularity of the core-cladding boundary and refractive index distribution fluctuations). Different models have been used to simulate these three important effects for SI optical fibers. The ray tracing model can determine the output angular power distribution while accounting for the mode-dependent attenuation. The time delay between individual rays can also be calculated in presence of modal dispersion. This model is computationally intensive because large number of ray-trajectories must be simulated. In contrast, the time-independent power flow equation [5] is effective in modeling mode-dependent attenuation, mode coupling, and how these influence the output angular power distribution with fiber length for different launch conditions. However, the frequency response and bandwidth are not calculated.

We have overcome this limitation using the time-dependent power flow equation and have determined the POF frequency response and bandwidth in addition to mode coupling and mode-dependent attenuation. Verified against measurements by Mateo et al. [6], we showed how the resulting change in bandwidth with fiber length is strongly affected by mode coupling typical of POFs.

2. Time-dependent power flow equation

We use Gloge's time-dependent power flow equation to describe the evolution of the modal power distribution along the axis of the SI POF (as the z-coordinate). Individual modes are characterized by their inner propagation angle θ measured with respect to fiber axis. Gloge's time-dependent power flow equation can be written as [7]:

$$\frac{\partial P(\theta,z,t)}{\partial z}+\frac{\partial t}{\partial z}\frac{\partial P(\theta,z,t)}{\partial t}=-\alpha(\theta)P(\theta,z,t)+\frac{1}{\theta}\times\frac{\partial}{\partial\theta}\left[\theta D(\theta)\frac{\partial P(\theta,z,t)}{\partial\theta}\right] \quad (1)$$

where t is the time, $P(\theta,z,t)$ is the power distribution over angle, space and time, respectively, $\alpha(\theta)$ is the mode-dependent attenuation,

* Corresponding author. Fax: +381 34 335040.
E-mail address: savovic@kg.ac.rs (S. Savović).

0143-8166/$ - see front matter © 2011 Elsevier Ltd. All rights reserved.
doi:10.1016/j.optlaseng.2011.01.016

$\partial t/\partial z$ is the mode delay per unit length and $D(\theta)$ is the mode-dependent coupling coefficient. Mode-dependent attenuation can be written in the form $\alpha(\theta)=\alpha_0+A\theta^2+...$, where α_0 is loss common to all modes. It can be accounted for by multiplying the end-solution by $e^{-\alpha_0 z}$ [8]. Therefore, in solving Eq. (1), one needs only to consider the term $A\theta^2$ as the most dominant of the higher order modes [5]. Assuming that the coupling coefficient D is mode-independent, Eq. (1) can be written as [7]:

$$\frac{\partial P(\theta,z,t)}{\partial z}+\frac{\partial t}{\partial z}\frac{\partial P(\theta,z,t)}{\partial t}=-A\theta^2P(\theta,z,t)+\frac{D}{\theta}\times\frac{\partial}{\partial\theta}\left[\theta\frac{\partial P(\theta,z,t)}{\partial\theta}\right] \tag{2}$$

The derivative $\partial t/\partial z$ can be obtained using the group velocity of a mode with characteristic angle θ, which is:

$$\frac{dz}{dt}=\frac{c}{n(1+\theta^2/2)} \tag{3}$$

Neglecting the delay n/c common to all modes, it follows [7]:

$$\frac{\partial P}{\partial z}=-A\theta^2P-\frac{n}{2c}\theta^2\frac{\partial P}{\partial t}+\frac{D}{\theta}\times\frac{\partial}{\partial\theta}\left(\theta\frac{\partial P}{\partial\theta}\right) \tag{4}$$

By applying the Laplace transform:

$$p(\theta,z,s)=\int_0^\infty e^{-st}P(\theta,z,t)dt \tag{5}$$

the time-dependent Eq. (4) transforms into an expression that differs from the following Gloge's [5] time-independent power flow Eq. (6) only in the multiplier A that is $A\sigma^2$ in Eq. (6):

$$\frac{\partial p}{\partial z}=-A\sigma^2\theta^2p+\frac{D}{\theta}\times\frac{\partial}{\partial\theta}\left(\theta\frac{\partial p}{\partial\theta}\right) \tag{6}$$

where $\sigma=(1+ns/2cA)^{1/2}$. Therefore, by substituting A in Eq. (4) with $A\sigma^2$, the solution of the time-dependent power flow Eq. (4) is obtained from the solution of the time-independent power flow Eq. (6).

For the Gaussian input distribution:

$$p_{in}=f(0,s)\exp[-\theta^2/\Theta_0^2] \tag{7}$$

one obtains [5]:

$$p(\theta,z,s)=f(z,s)\exp[-\theta^2/\Theta^2(z,s)] \tag{8}$$

where $\Theta^2(z,s)$ and $f(z,s)$ are described by [5]:

$$\Theta^2(z,s)=\frac{\Theta_\infty^2}{\sigma}\frac{\sigma\Theta_0^2+\Theta_\infty^2\tan h\sigma\gamma_\infty z}{\Theta_\infty^2+\sigma\Theta_0^2\tan h\sigma\gamma_\infty z} \tag{9}$$

and

$$f(z,s)=\frac{f(0,s)\sigma\Theta_0^2}{\Theta_\infty^2\sin h\sigma\gamma_\infty z+\sigma\Theta_0^2\cos h\sigma\gamma_\infty z} \tag{10}$$

with

$$\Theta_\infty=(4D/A)^{1/4} \tag{11}$$

and

$$\gamma_\infty=2(AD)^{1/2} \tag{12}$$

For continuous wave excitation ($s=0$), the angular width $\Theta(z,0)$ changes monotonically from Θ_0 to Θ_∞ as z increases. Since the width Θ_∞ characterizes a distribution, which propagates unchanged (at steady state) and with the minimum overall loss coefficient γ_∞, it seems practical to excite this distribution right from the beginning ($\Theta_0=\Theta_\infty$) [7]. The closed-form Laplace transform of Eq. (8) exists only for the approximation given in the limits $z\ll 1/\gamma_\infty$ (short fiber) and $z\gg 1/\gamma_\infty$ (long fibers) [7].

For short fibers, Eq. (8) becomes [7]:

$$p(\theta,z,s)=\frac{f(0,s)}{1+\gamma_\infty z}\exp\left[-\theta^2\left(\frac{1}{\Theta_0^2}+\frac{nz}{2c}s\right)\right] \tag{13}$$

The total output is obtained from the integration $p(\theta,z,s)$ over all angles [7]. With reference to Eq. (13) and for $z\ll 1/\gamma_\infty$, one obtains:

$$q=\frac{\pi f(0,s)\Theta_0^2}{(1+\gamma_\infty z)(1+n\Theta_0^2zs/2c)} \tag{14}$$

If one sets$f(0,s)=1$, which corresponds to an infinitesimally short input pulse of energy 1, the Laplace transformation of Eq. (14) yields the impulse response of the fiber [7]:

$$Q(z,t)=\frac{2c\pi}{nz(1+\gamma_\infty z)}\exp(-2ct/n\Theta_0^2z) \tag{15}$$

where $Q(t)$ is limited in practice to a time interval narrower than $n\theta_c^2z/(2c)$, which is the delay between the fastest and the slowest modes (θ_c is the fiber's critical angle).

In the case of a long fiber, Eq. (8) assumes the form [7]:

$$p=\frac{2\sigma}{1+\sigma}\exp\left[-\sigma(\theta^2/\Theta_0^2+\gamma_\infty z)\right] \tag{16}$$

which leads to:

$$q=\frac{2\pi\Theta_0^2}{1+\sigma}\exp(-\sigma\gamma_\infty z) \tag{17}$$

where p is integrated over all angles θ. Introducing $\sigma=(1+ns/2cA)^{1/2}$ into Eq. (17), one can form the Laplace transform of $q(s)$. By using the condition $\gamma_\infty z>1$, the impulse response of the fiber is:

$$Q(z,t)=\Theta_0^2\sqrt{\frac{\pi}{Tt}}\left(\frac{t}{\gamma_\infty zT}+\frac{1}{2}\right)^{-1}\exp\left(-\frac{\gamma_\infty^2z^2T}{4t}-\frac{t}{T}\right) \tag{18}$$

where

$$T=\frac{n}{2cA}=\frac{n}{2c}\times\frac{\Theta_0^2}{\gamma_\infty} \tag{19}$$

After obtaining impulse response, frequency response can be obtained easily by applying Fourier transform to the impulse response:

$$H(f)=\int_{-\infty}^{+\infty}Q(t)\exp(-2\pi ift)dt \tag{20}$$

In addition to Gloge's analytical solution for the time-dependent power flow Eq. (2) [7], two numerical approaches for solving the time-dependent power flow Eq. (1) have also been reported. They are the implicit finite-difference method (Crank-Nicholson scheme) by Breyer et al. [9] and explicit finite-difference method in the matrix form by Mateo et al. [6]. In this work, to our knowledge for the first time, using Gloge's analytical solution of Eq. (2), we calculate the impulse response, frequency response and bandwidth of the SI POF investigated earlier by Mateo et al. [6] and compare our analytical to their experimental results. One should mention here that numerical approaches in solving Eq. (2) [6,9] are often very complex and computationally more difficult to perform, so application of the analytical solution of the problem is always more convenient if such solution exists.

3. Results

It was shown in the preceding Section how the time-dependent analysis is reduced to its time-independent equivalent. This is applied to calculate the impulse response, frequency response and bandwidth of the SI POF that was investigated by Mateo et al. [6]. This fiber is the PGU-FB1000 (PGU) from Toray with numerical aperture NA=0.5 (corresponding to the inner critical angle of $\theta_c=19.5^\circ$) and 0.15 dB/m of nominal attenuation. Mateo et al. [6] measured frequency responses at different fiber lengths by feeding pure sinusoidal waveforms of different frequencies to an AlGaInP laser diode (LD Sanyo DL-3147-021). The laser source

emits a maximum power of 5 mW at 645 nm and has a typical divergence of 30° in the perpendicular plane, and 7.5° in the parallel plane. Power was launched directly into the fiber using a connector, which limits the NA to near 0.19 (under-filled launch) but is close to the conditions achieved in real links. The receptor is based on a 1 mm diameter photodiode (FDS010) with a 50 Ω load resistance and whose bandwidth is 200 MHz. The fiber-output is free-space coupled to the receptor using another connector. Most of the power is captured due to the large area of the detector, avoiding spatial filtering that could modify measured frequency responses. The receptor output is amplified using a 40 dB amplifier (Mini-Circuits ZKL-1R5) with a band-pass from 10 MHz to 1.5 GHz. A wideband Infinium DCA 86100A oscilloscope from Agilent is connected to the output of the amplifier and captures the received signal whose amplitude is directly related with the frequency response of the system at that frequency. Device control and data acquisition are performed by the computer. The detailed procedure to obtain the frequency response is described in [6] and references within. In calculating the impulse response and frequency response of PGU fiber, Mateo et al. [6] have assumed mode-dependent attenuation $\alpha(\theta)$ and mode-dependent coupling coefficient $D(\theta)$. In contrast, Gloge's analytical solution of the time-dependent power flow Eq. (2) is obtained assuming a constant coupling coefficient D and constant A (A is the second order multiplicative factor in the series expansion of the mode-dependent attenuation $\alpha(\theta)$). In order to obtain the value for A for the fiber in question, we used the graph for $\alpha(\theta)$ in Fig. 1 proposed earlier for PGU fiber by Mateo et al. [10]. Since mode-dependent attenuation can be written in the form $\alpha(\theta) \approx \alpha_0 + A\theta^2$, one can determine A by fitting the graph of Fig. 1 using this $\alpha(\theta)$ function. In doing so, we have obtained $\alpha_0 = 0.015\ \mathrm{m}^{-1}$ and $A = 0.9953\ (\mathrm{rad}^2\ \mathrm{m})^{-1}$. On the basis of the distribution of mode-dependent coupling coefficient $D(\theta)$ proposed earlier for PGU fiber by Mateo et al. [10] (Fig. 2), we have obtained that the value of the coupling coefficient $D \approx 5.02 \times 10^{-4}\ \mathrm{rad}^2/\mathrm{m}$ characterizes mode coupling in the angular range of interest $\theta \approx 0$ to 7° (in the calculations we assumed that the light beam is launched centrally along the fiber axis with FWHM = 10.2°). One should mention here that modeling the mode coupling process with a constant D is commonly done by many other authors [5, 11–15].

A Dirac impulse in time and a mode distribution with the width at $1/e$ of $\Theta_0 = \Theta_\infty = 12°$ (FWHM = 10.2°) at the beginning of the fiber are used (Mateo et al. [6] used a laser diode with FWHM = 7.5° in the parallel plane). Eq. (8), valid for long fiber lengths $z \gg 1/\gamma_\infty = 22.4$ m, has been used to calculate the impulse response at fiber lengths $z = 50$, 100 and 150 m. Our analytical results for the impulse response for different fiber lengths of the PGU fiber are shown in Fig. 3. In Fig. 4, experimental results obtained by Mateo et al. [6] for impulse response are shown for the fiber length of 150 m. A good agreement between these results is apparent. The tail beyond 20 ns of the experimentally obtained impulse response [6] at the end of 150 m PGU fiber length seems longer than our analytical results and possibly is due to the noticeable difference in the attenuation functions as shown in Fig. 1. One can observe from Fig. 3 that at short fiber lengths, the mode-dependent attenuation and modal dispersion are the dominant effects. With increasing fiber length, mode coupling begins to influence significantly the impulse shape, changing it to a more or less Gaussian shape. The power exiting the fiber at the highest angles (the tails of the Gaussian launch beam) is delayed the most. This suggests an efficient means of improving the fiber performance by spatially filtering-out of the tail-ends at higher angles [6]. As most power is confined within the range of lower angles, such filtering of the power at highest angles would cause only minor power loss while producing a narrower overall impulse response.

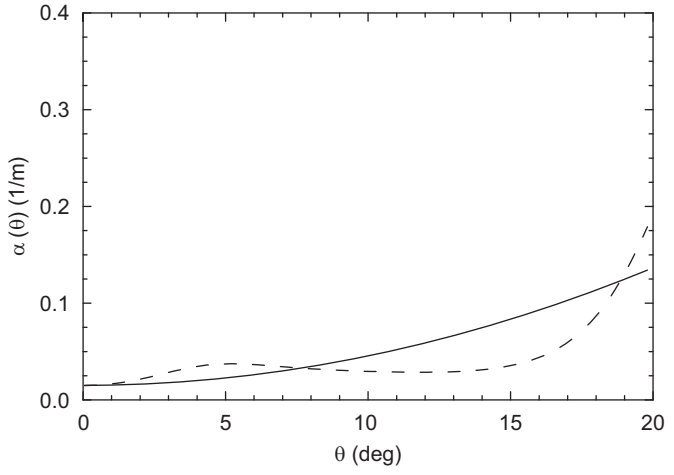

Fig. 1. Mode-dependent attenuation $\alpha(\theta)$ for PGU fiber proposed by Mateo et al. [10] (dashed line) and our fit obtained using the function $\alpha(\theta) \approx \alpha_0 + A\theta^2$, with $\alpha_0 = 0.015\ \mathrm{m}^{-1}$ and $A = 0.9953\ (\mathrm{rad}^2\ \mathrm{m})^{-1}$ (solid line).

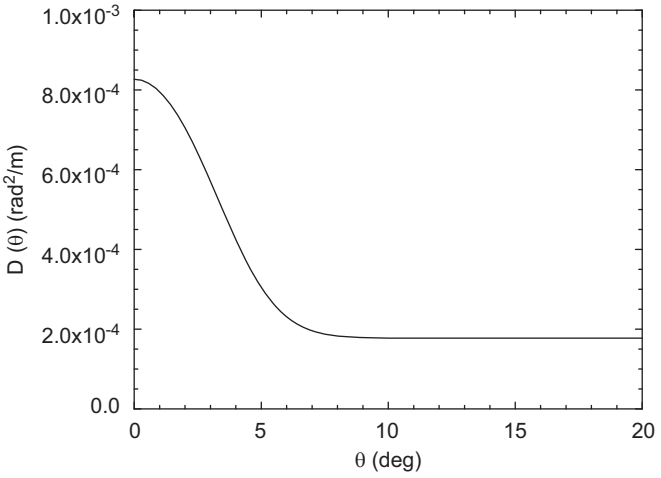

Fig. 2. Mode-dependent coupling coefficient $D(\theta)$ for PGU fiber proposed by Mateo et al. [10].

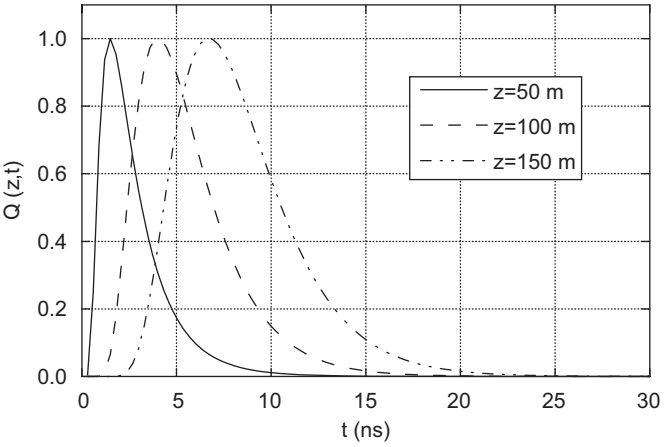

Fig. 3. Analytical results for the impulse response for different fiber lengths for PGU fiber.

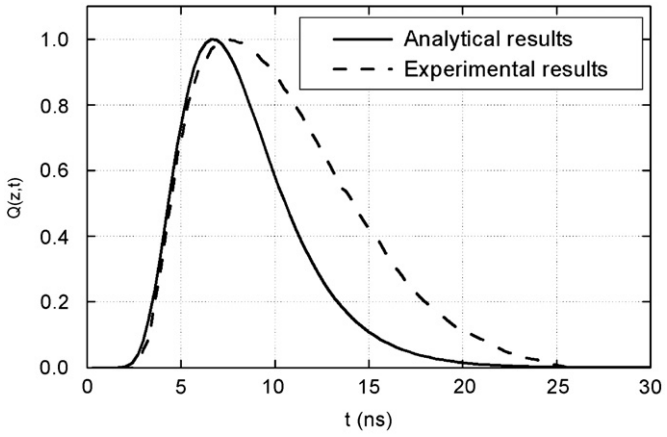

Fig. 4. Experimental results for the impulse response at the end of 150 m PGU fiber length obtained by Mateo et al. [6] compared with our analytical results.

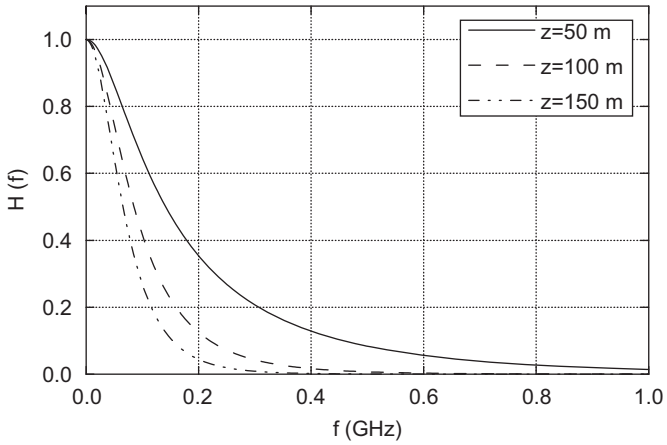

Fig. 5. Analytical results for the frequency response for different fiber lengths for PGU fiber.

Fig. 5 shows frequency response of the PGU fiber obtained using Eq. (9). The low frequency performance differs from that at high frequencies. Moreover, a more pronounced drop at lower frequencies is apparent for longer fiber length. A similar frequency response has been observed for HFB POF investigated by Mateo et al. [6].

In Fig. 6, Mateo's and our results are compared and show a good match for the bandwidth. The differences between these results at short fiber lengths can be explained by the fact that in our calculations the launch mode distribution with FWHM$=10.2^{\circ}$ is used while Mateo et al. [6] in the experiment used a laser diode with FWHM$=7.5^{\circ}$. Namely, influence of the width of the launched beam on the evolution of the width of the output angular power distribution, and consequently on the fiber bandwidth, is more pronounced at short fiber lengths [16], leading to the underestimated analytically obtained bandwidth. With increasing fiber length this influence becomes negligible. One can also see that bandwidth decreases with length more steeply for shorter fiber lengths. POF bandwidth as a function of fiber length (in logarithmic coordinates) has usually been approximated by straight lines. The slope of these lines is known as the concatenation factor and is related to mode coupling. In the absence of mode coupling and differential mode attenuation, the concatenation factor is unity. Therefore, a slope higher or lower than this is evidence of diffusive non-linear effects [6]. Mateo et al. [6] showed that the bandwidth data for the PGU fiber

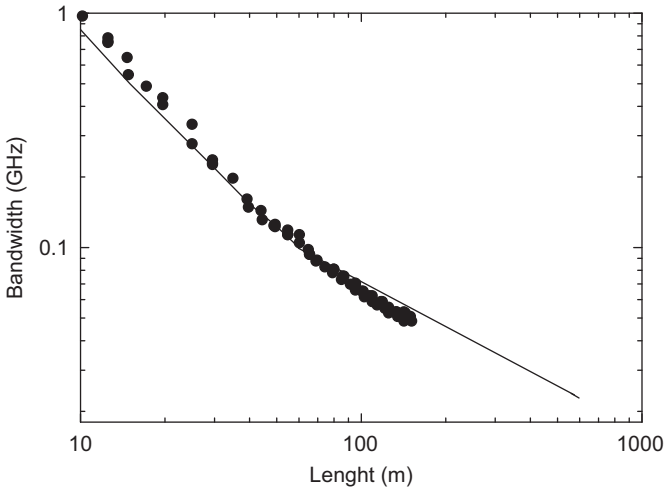

Fig. 6. Analytical results for the bandwidth versus fiber length for PGU fiber (line) compared to experimental results (symbols) obtained by Mateo et al. [6]. Line shows model predictions extended up to 600 m.

can be fitted with two lines intercepting at about 60 m, with a slope of 1.3 for the first and 0.8 for the second line. Slope above unity is caused by under-filled launch. Combined with modal diffusion, it degrades the overall fiber performance by causing faster drop in bandwidth. The segment with a slope of 0.8 is indicative of stronger modal diffusion that leads to the equilibrium distribution faster. Thus, one can conclude that at the fiber length of about 60 m, weakly coupled regimes become strongly coupled beyond the coupling length L_c (the fiber length where equilibrium mode distribution is achieved) [15].

4. Conclusion

The analytical solution of the time-dependent power flow equation is employed for the first time to calculate the impulse response, frequency response and bandwidth in a step-index plastic optical fiber that was investigated experimentally by Mateo et al. [6]. Our results for the impulse response agree well with experiments [6]. It has been observed that at short fiber lengths the mode-dependent attenuation is dominant. With increasing fiber length, mode coupling begins to influence the impulse response of the fiber, which begins to take the Gaussian-like shape. Frequency response at a range of lengths enabled us to derive the bandwidth dependence on distance. A good agreement between our results and experimental results from the literature [6] is obtained. One could observe that the switch from weakly to strongly coupled regimes results in the slower drop of bandwidth for fibers longer than the coupling length L_c, which means that mode coupling enhances the fiber bandwidth.

Acknowledgement

The work described in this paper was supported by the grant from the Serbian Ministry of Science and Technological Development (Project no. 171011).

References

[1] Ishigure T, Kano M, Koike Y. Which is a more serious factor to the bandwidth of GI POF: differential mode attenuation or mode coupling? J Lightwave Technol 2000;18:959–65.

[2] Golowich SE, White W, Reed WA, Knudsen E. Quantitative estimates of mode coupling and differential modal attenuation in perfluorinated graded-index plastic optical fiber. J Lightwave Technol 2003;21:111–21.
[3] Green Jr. PE. Optical networking update. IEEE J Sel Areas Commun 1996;14:764–79.
[4] Koeppen C, Shi RF, Chen WD, Garito AF. Properties of plastic optical fibers. J Opt Soc Am B 1998;15:727–39.
[5] Gloge D. Optical power flow in multimode fibers. Bell Syst Tech J 1972;51: 1767–83.
[6] Mateo J, Losada MA, Zubía J. Frequency response in step index plastic optical fibers obtained from the generalized power flow equation. Opt Express 2009;17:2850–60.
[7] Gloge D. Impulse response of clad optical multimode fibers. Bell Syst Tech J 1973;52:801–16.
[8] Savović S, Djordjevich A. Influence of numerical aperture on mode coupling in step index plastic optical fibers. Appl Opt 2004;43:5542–6.
[9] Breyer F, Hanik N, Lee J, Randel S. Getting impulse response of SI-POF by solving the time-dependent power-flow equation using Cranck-Nicholson scheme. In: Bunge C-A, Poisel H, editors. Proceedings of the POF Modelling Workshop, 24–28 June, Nurneberg, Germany, 2007, p. 111–9.
[10] Mateo J, Losada MA, Garcés I, Zubía J. Global characterization of optical power propagation in step-index plastic optical fibers. Opt Express 2006;14: 9028–35.
[11] Gambling WA, Payne DN, Matsumura H. Mode conversion coefficients in optical fibers. Appl Opt 1975;14:1538–42.
[12] Dugas J, Maurel G. Mode-coupling processes in polymethyl methacrylate-core optical fibers. Appl Opt 1992;31:5069–79.
[13] Rousseau M, Jeunhomme L. Numerical solution of the coupled-power equation in step index optical fibers. IEEE Trans Microwave Theory Tech 1977;25:577–85.
[14] Jeunhomme L, Fraise M, Pocholle JP. Propagation model for long step-index optical fibers. Appl Opt 1976;15:3040–6.
[15] Garito AF, Wang J, Gao R. Effects of random perturbations in plastic optical fibers. Science 1998;281:962–7.
[16] Savović S, Djordjevich A, Tse PW, Zubia J, Mateo J, Losada MA. Determination of the width of the output angular power distribution in step index multi-mode optical fibers. J Opt 2010;12(115405):5.